Tracking Improvements for Nonlinear Systems Using Inversion-Based Feedforward Control and Feedback Control: A Robotic Arm Example

Jiradech Kongthon
Department of Mechatronics Engineering, Assumption University, Samutprakan, Thailand
Email: jiradechkng@au.edu

***Abstract*—This article seeks approaches to controlling the motion of a robotic arm that needs to follow a given time-profile trajectory within a required time period. The equation of motion of the robotic arm is derived and it exhibits a nonlinear behavior. This work proposes three different control methods: (i) feedback control approach, (ii) inversion-based feedforward control, and (iii) integration of feedforward control with feedback control. Each control approach is simulated to track time-profile trajectories. The tracking performance for each controller is evaluated through tracking errors. The contributions of this research work are to demonstrate that: (i) the feedback approach cannot properly track the trajectories, and tracking errors may be unacceptable in some applications, (ii) the feedforward approach can substantially enhance the tracking performance, compared to that of the feedback method, and (iii) integration of feedforward control with feedback control method can further improve the tracking and achieve the best tracking performance. The integration of feedforward control method with feedback control approach can perhaps be effectively implemented when very good tracking is required.**

***Index Terms*—feedback control, feedforward control, inversion-based control, manipulator, robotic arm, trajectory tracking, perturbation, relative degree**

I. Introduction

Tracking a trajectory is required when the goal is to move an object to follow a time-profile trajectory within an acceptable error. Several works have achieved good tracking. Some examples are the works in [1]-[7].

Tracking a trajectory could be challenging for a nonlinear system as tools for nonlinear control are not plenty, compared to tools available for linear control systems. The tracking could be even more challenging when the robustness of control is required to handle the modeling errors or the perturbation.

The developments of manipulators, or robotic arms have been made for many decades, and the control methods to move the arms have been achieved in many works presented in the literature. For example, the work in [8] used an auto-tuning PID controller to regulate a flexible manipulator. The work presented in [9] implemented a position control for manipulators based on the principle of orthogonal decomposition spaces by holonomic constraints. Controllers used to counteract both uncertain dynamics and unbounded disturbances to a robotic manipulator were proposed in [10]. The research in [11] presented the trajectory tracking control and the vibration control of the robotic manipulator with the input constraint using a dual-loop iterative learning control law.

This work seeks approaches to controlling the motion of a robotic arm that needs to follow a given time-profile trajectory within a required time. The equation of motion of the robotic arm is derived and it exhibits a nonlinear behavior. This work proposes three different control methods: (i) feedback control approach, (ii) inversion-based feedforward control, and (iii) integration of feedforward control with feedback control. Each control approach is simulated to track time-profile trajectories. The study also includes the tracking under perturbations, or modeling errors and the tracking of faster trajectories. The tracking performance for each controller is evaluated through tracking errors. The tracking results show that (i) using the feedback control alone cannot yield good tracking, and tracking with the feedback control alone gets worse when the trajectory gets faster, or there is a modeling error, or perturbation in the system, (ii) using the feedforward control alone can substantially improve the tracking although the trajectory gets faster, or there is a modeling error, or perturbation in the system, and (iii) the integration, or combination of the feedforward control method with the feedback control approach can further improve the tracking and can achieve the best tracking performance. The combined controller can produce good tracking of the fast system under perturbations.

II. System Equation of Motion and Trajectory

A. System Equation of Motion

In this work, a robotic arm, or manipulator of one degree of freedom shown in Fig. 1 is considered.

Manuscript received December 14, 2018; revised October 5, 2019.

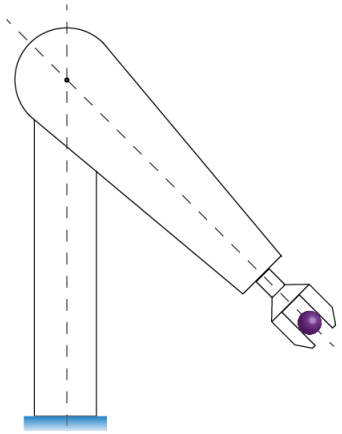

Figure 1. Robotic *arm*.

The mathematical model of the system can be obtained by applying Newton's laws of motion. It is noted that one can take an alternative approach to obtaining the equation of motion. To work with the Newtonian approach, the free body diagram of the body of interest must be drawn as it is shown in Fig. 2.

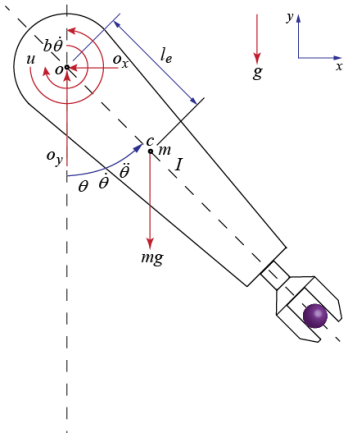

Figure 2. Free body diagram of the robotic arm.

In the free body diagram, the following notations, or symbols are assigned and described as follows.

g represents the gravitational acceleration.

m represents the total effective mass of the arm that includes the mass of the load at the gripper.

mg represents the total effective weight of the arm that includes the weight of the load at the gripper.

I represents the total effective mass moment of inertia about the axis passing through point O , and it includes the inertia of the load at the gripper.

l_e represents the effective distance measured from the center of rotation (point O) to the center of the effective mass (point C).

o_x and o_y represent the reaction forces at point O in the x-component and the y-component respectively.

θ represents the angular position of the arm.

$\dot{\theta}$ represents the angular velocity of the arm.

$\ddot{\theta}$ represents the angular acceleration of the arm.

u represents the input, which is the torque applied to move the arm.

$b\dot{\theta}$ represents the viscous damping torque due to the friction at joint O and b represents the damping coefficient.

By reading the free body diagram and taking the moment about point O, the moment equation of motion is written below.

$$-(mg\sin\theta)l_e - b\dot{\theta} + u = I\ddot{\theta} \tag{1}$$

It is obvious that the equation of motion expressed in (1) is nonlinear.

B. *Trajectory*

To dictate the motion of the arm over time, a time profile trajectory $\theta(t)$ is defined. The control goal is to move the arm including the load to follow the time profile trajectory given.

To determine a time profile trajectory $\theta(t)$, the corresponding angular acceleration $\ddot{\theta}(t)$ may be chosen as

$$\ddot{\theta}(t) = A\sin(\frac{2\pi t}{T}) = \frac{d}{dt}\dot{\theta}(t),\ t_1 \le t \le t_1 + T$$

$$\ddot{\theta}(t) = 0,\ \ t < t_1 \ \text{ and } \ t > t_1 + T$$

where A represents the amplitude and T denotes the time period of the desired motion.

By integration, the angular velocity $\dot{\theta}(t)$ is obtained as follows.

$$\dot{\theta}(t) = -\frac{AT}{2\pi}\left[\cos(\frac{2\pi t}{T}) - 1\right] = \frac{d}{dt}\theta(t)$$

It is assumed that in this work, the maximum output $\theta_{,\max}$ = 1 rad. The corresponding angular position θ is then obtained by integration.

$$\theta(t) = \frac{ATt}{2\pi} - \frac{AT^2}{(2\pi)^2}\sin(\frac{2\pi t}{T})$$

The plots of the angular acceleration $\ddot{\theta}(t)$, the angular velocity $\dot{\theta}(t)$, the angular position $\theta(t)$ against time (in second) for T = 0.5 s and t_1= T/2 are illustrated below.

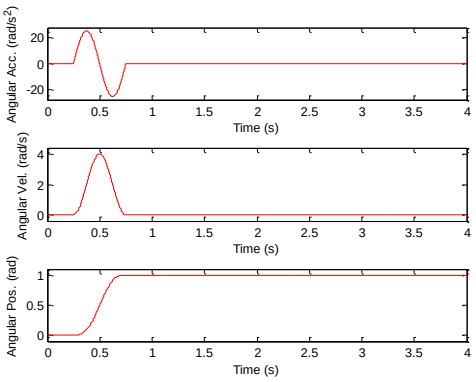

Figure 3. Position, velocity, and acceleration for T = 0.5 s.

It is observed that in the top figure of Fig. 3, there are two sharp corners for the acceleration time profile. This will lead to poor tracking. To solve this issue, the trajectory needs to be smoothened by a second-order filter described by the following transfer function $G_f(s)$.

$$G_f(s) = \left(\frac{\omega_f}{s + \omega_f} \right)^2$$

where ω_f denotes the break frequency of the filter, and in this study, ω_f of 30 Hz, or $30(2\pi)$ rad/s is used to smoothen the trajectory. Hereafter, the smoothened time-profile trajectory is referred to as the desired trajectory, and it is denoted with a subscript *d* (such as θ_d). Hence, the control schemes are to track the desired trajectory.

III. System Model and Control Approaches

From the equation of motion expressed in (1), the state variables (x_1 and x_2) of the system can be assigned to be the angular position θ and the angular velocity $\dot{\theta}$; i.e.,

$$x = \begin{bmatrix} x_1 \\ x_2 \end{bmatrix} = \begin{bmatrix} \theta \\ \dot{\theta} \end{bmatrix} \tag{2}$$

From the state variables in (2) and the equation of motion in (1), the state equation can be written as shown below.

$$\dot{x} = \begin{bmatrix} \dot{x}_1 \\ \dot{x}_2 \end{bmatrix} = \begin{bmatrix} \dot{\theta} \\ \ddot{\theta} \end{bmatrix} = \begin{bmatrix} \dot{\theta} \\ (-(mg\sin\theta)l_e - b\dot{\theta} + u)/I \end{bmatrix} \tag{3}$$

Equation (3) can be represented by a single-input nonlinear state space representation of the form (as in [12])

$$\dot{x} = f(x) + g(x)u \tag{4}$$

It is noted that the standard form of the system output equation is

$$y = h(x) \tag{5}$$

Hence, by observing the standard form in (4), the nonlinear state equation in (3) is rewritten as

$$\dot{x} = \begin{bmatrix} x_2 \\ (-mgl_e \sin x_1 - bx_2)/I \end{bmatrix} + \begin{bmatrix} 0 \\ 1/I \end{bmatrix} u \tag{6}$$

Since the goal is to track the trajectory θ, the output equation is dictated to be

$$y = h(x) = \begin{bmatrix} 1 & 0 \end{bmatrix} x = x_1 \tag{7}$$

Therefore, the system is described by the following equations.

$$f(x) = \begin{bmatrix} x_2 \\ (-mgl_e \sin x_1 - bx_2)/I \end{bmatrix} \tag{8}$$

$$g(x) = \begin{bmatrix} 0 \\ 1/I \end{bmatrix} \tag{9}$$

$$h(x) = \begin{bmatrix} 1 & 0 \end{bmatrix} \begin{bmatrix} x_1 \\ x_2 \end{bmatrix} \tag{10}$$

In this study, three control schemes are presented and proposed to track the desired trajectory: (i) feedback control, (ii) feedforward control, and (iii) combination of feedback control scheme and feedforward control approach.

A. Feedback Control

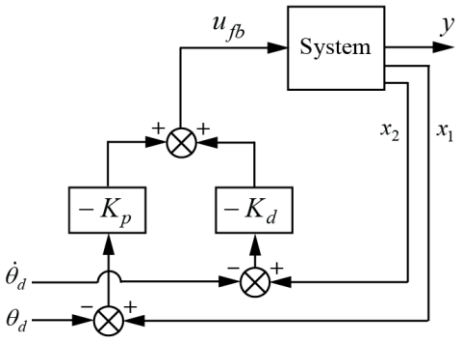

Figure 4. Block diagram of feedback control.

The method of feedback control is extensively used to regulate output motions and there are several feedback control methods such as PID control schemes, linear-quadratic-gaussian regulator control (LQG), linear-quadratic regulator control (LQR) as in [13] and [14], etc. In this work, a PD controller is used to track the desired trajectories. The PD state feedback (as in [14]) is described by the block diagram in Fig. 4.

From Fig. 4, the state feedback law is written as

$$u_{fb} = -k_p(x_1 - \theta_d) - k_d(x_2 - \dot{\theta}_d) \tag{11}$$

where u_{fb} is the feedback input, and k_p and k_d are the proportional gain and the derivative gain respectively.

It is noted that in this study, $k_p = 10$ Nm and $k_d = 10$ Nms are used.

The feedback control method is implemented to track the trajectories, and MATLAB software is used to simulate the system. The results are shown in Section IV.

B. Inversion-Based Feedforward Control

The theory and the development of inversion-based feedforward control have been around for several decades. The very early and great works on inversion-based control were proposed in [15]-[17]. The inversion-based feedforward control approach (as in [18]-[22]) is a powerful and effective approach for trajectory tracking problems where the trajectory is known a priori, and it has been implemented in plenty of works such as the works in [3]-[7]. The standard block diagram of the inversion-based feedforward control is shown in Fig. 5.

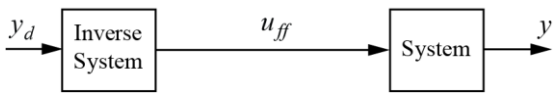

Figure 5. Block diagram of feedforward control.

To find the inverse control input in the inversion-based approach, it requires taking the *r*th time derivative till the control input appears. *r* is referred to as the relative degree.

Taking the first time derivative of the output equation shown in (7) by using Lie derivatives (as in [12]) yields

$$\dot{y} = L_f h(x) + [L_g h(x)]u \tag{12}$$

where $L_f h = \frac{\partial h}{\partial x} f = \begin{bmatrix} \frac{\partial h}{\partial x_1} & \frac{\partial h}{\partial x_2} \end{bmatrix} f$

$$= \begin{bmatrix} 1 & 0 \end{bmatrix} \begin{bmatrix} x_2 \\ (-mgl_e \sin x_1 - bx_2)/I \end{bmatrix}$$

Or,

$$L_f h = x_2 \tag{13}$$

And,

$$L_g h = \frac{\partial h}{\partial x} g = \begin{bmatrix} 1 & 0 \end{bmatrix} \begin{bmatrix} 0 \\ 1/I \end{bmatrix} = 0 \tag{14}$$

Substituting (13) and (14) into (12) leads to

$$\dot{y} = L_f h \tag{15}$$

Taking the second time derivative of the output equation shown in (7) by using Lie derivatives yields

$$\ddot{y} = L_f^2 h + [L_g L_f h]u \tag{16}$$

where $L_f^2 h = \begin{bmatrix} \frac{\partial (L_f h)}{\partial x} \end{bmatrix} f = \begin{bmatrix} \frac{\partial (x_2)}{\partial x} \end{bmatrix} f$

$$= \begin{bmatrix} 0 & 1 \end{bmatrix} \begin{bmatrix} x_2 \\ (-mgl_e \sin x_1 - bx_2)/I \end{bmatrix}$$

or,

$$L_f^2 h = (-mgl_e \sin x_1 - bx_2)/I \tag{17}$$

and,

$$L_g L_f h = \begin{bmatrix} \frac{\partial (L_f h)}{\partial x} \end{bmatrix} g = \begin{bmatrix} 0 & 1 \end{bmatrix} \begin{bmatrix} 0 \\ 1/I \end{bmatrix} = 1/I \neq 0 \tag{18}$$

At this point, it reveals that the relative degree is 2 as the input appears in (16) since $L_g L_f h \neq 0.$

Substituting (17) and (18) into (16) results in

$$\ddot{y} = L_f^2 h + [L_g L_f h]u \tag{19}$$

Or,

$$\ddot{y} = (-mgl_e \sin x_1 - bx_2)/I + (1/I)u \tag{20}$$

In terms of the angular position θ and the angular velocity $\dot{\theta}$, (20) can be written as

$$\ddot{y} = (-mgl_e \sin\theta - b\dot{\theta})/I + (1/I)u \tag{21}$$

In a tracking scenario of angular motions, it requires that $y = y_d = \theta_d$, so $\dot{y} = \dot{y}_d = \dot{\theta}_d$ and $\ddot{y} = \ddot{y}_d . = \ddot{\theta}_d$.

Hence, the inverse input u_{inv} can be solved from (21); i.e.,

$$u_{inv} = \frac{1}{1/I}[\ddot{y}_d - (-mgl_e \sin\theta - b\dot{\theta})/I] \tag{22}$$

In case of tracking the rotational motion,

$$y_d = \theta_d \ , \ \dot{y}_d = \dot{\theta}_d \quad \text{and} \quad \ddot{y}_d = \ddot{\theta}_d$$

Hence in (22), the inverse input u_{inv} , or the feedforward input u_{ff} can be written as

$$u_{inv} = \frac{1}{1/I}[\ddot{y}_d - (-mgl_e \sin y_d - b\dot{y}_d)/I] \tag{23}$$

or,

$$u_{inv} = u_{ff} = I\ddot{\theta}_d + mgl_e \sin\theta_d + b\dot{\theta}_d \tag{24}$$

In the simulations in Section IV, the following values are used:

$$mgl_e = 1\,\text{Nm}, \ b = 1\,\text{Nms}, \text{ and } I = 1\,\text{kgm}^2$$

In the study of perturbations, the value of $I = 1\,\text{kgm}^2$ will be changed to $I = 1.2\,\text{kgm}^2$ (20% increase, or error) to account for modeling errors, or perturbations studied in Section IV.

The feedforward control scheme is applied to track the trajectories, and MATLAB software is used to simulate the system. The tracking results are shown in Section IV.

C. Integration of Feedback Control with Feedforward Control

The work in [23] combined the feedforward control with the feedback control method to improve the control performance. To further improve the tracking performance, this work also proposes a control method that integrates the feedforward control with the feedback control. The control scheme is illustrated in Fig. 6 below.

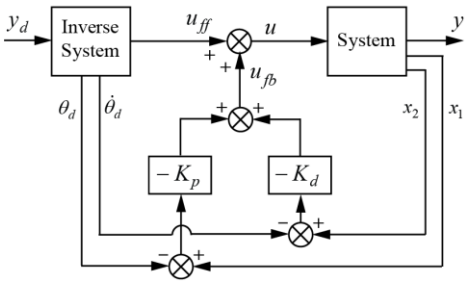

Figure 6. Block diagram of feedback-feedforward control: Integration of feedforward control with feedback control.

There are several options for feedback controller design. Here, the PD controller is chosen as discussed in Subsection *A* of Section III, and from Fig. 6, the feedback input u_{fb} is determined (as in (11)).

$$u_{fb} = -k_p(x_1 - \theta_d) - k_d(x_2 - \dot{\theta}_d) \tag{25}$$

u_{ff} , or u_{inv} is obtained from (24) in Subsection *B* of Section III.

The total input u can then be determined as

$$u = u_{ff} + u_{fb} \tag{26}$$

The combined control scheme is implemented to track the trajectories, and MATLAB software is used to

simulate the system. The results of tracking are shown in Section IV.

IV. Results and Discussions

This section presents the results obtained from the MATLAB simulations. The following parameters, or values are used in the simulations.

$\omega_f = 30\,\text{Hz} = 30(2\pi)\,\text{rad/s}$, $\theta_{\max} = 1\,\text{rad}$, $mgl_e = 1\,\text{Nm}$, $b = 1\,\text{Nms}$, $k_p = 10\,\text{Nm}$, and $k_d = 10\,\text{Nms}$, $I = 1\,\text{kgm}^2$, and $T = 1\,\text{s}$.

In the study of the system under perturbations, the value of $I = 1\,\text{kgm}^2$ is changed to $I = 1.2\,\text{kgm}^2$ (20% increase, or error) to account for modeling errors, or perturbations. The study indicates the robustness of the control approach to ensure that under perturbations due to the modeling errors, or the variation in the loading, the tracking is still acceptable.

Furthermore, to investigate the effectiveness and performance of tracking a faster trajectory, the value of $T = 1\,\text{s}$ is changed to $T = 0.5\,\text{s}$ (50% faster).

With the zero initial conditions for all the states at time $t = 0$, the results of tracking are shown in Fig. 7 to Fig. 18.

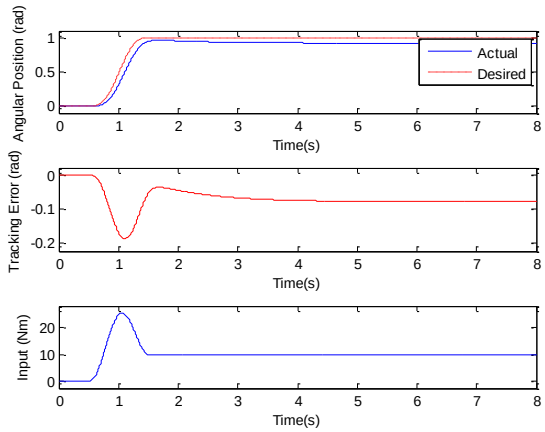

Figure 7. Top: Actual position θ_a and desired position θ_d. Middle: Tracking error $\theta_a - \theta_d$. Bottom: Input, using feedback control alone, I =1.0 kgm^2, T = 1 s.

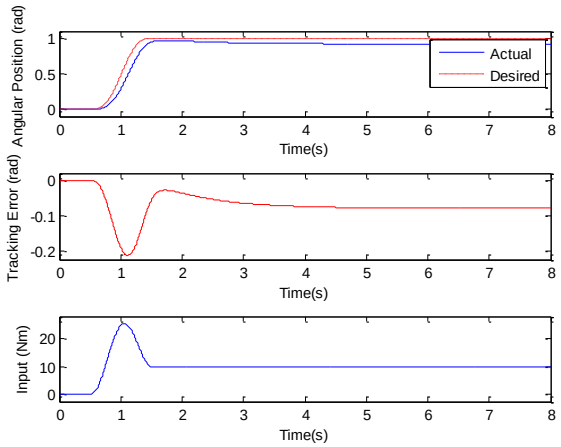

Figure 8. Top: Actual position θ_a and desired position θ_d. Middle: Tracking error $\theta_a - \theta_d$. Bottom: Input, using feedback control alone, I =1.2 kgm^2, T = 1 s.

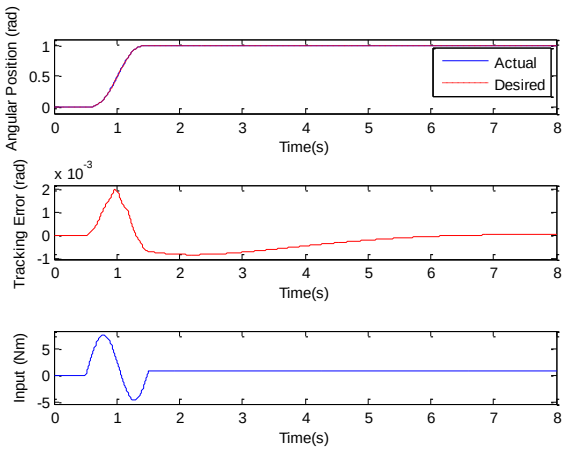

Figure 9. Top: Actual position θ_a and desired position θ_d. Middle: Tracking error $\theta_a - \theta_d$. Bottom : Input , using feedforward control alone, I =1.0 kgm^2, T = 1 s.

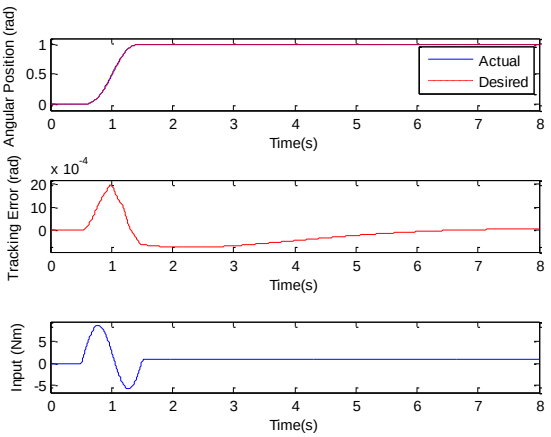

Figure 10. Top: Actual position θ_a and desired position θ_d. Middle: Tracking error $\theta_a - \theta_d$, Bottom : Input, using feedforward control alone, I =1.2 kgm^2, T = 1 s.

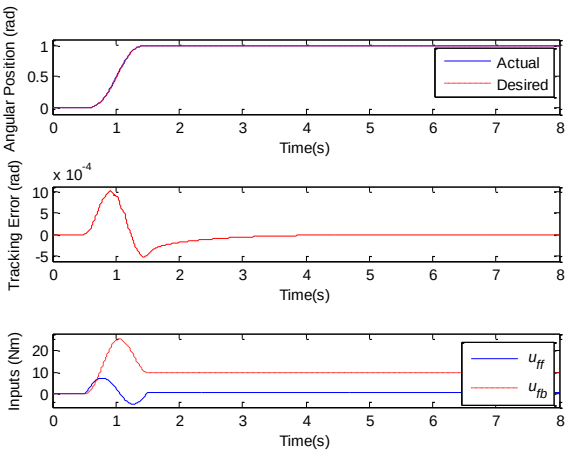

Figure 11. Top: Actual position θ_a and desired position θ_d. Middle: Tracking error $\theta_a - \theta_d$. Bottom: Inputs, using feedback control and feedforward control, I =1.0 kgm^2, T = 1 s.

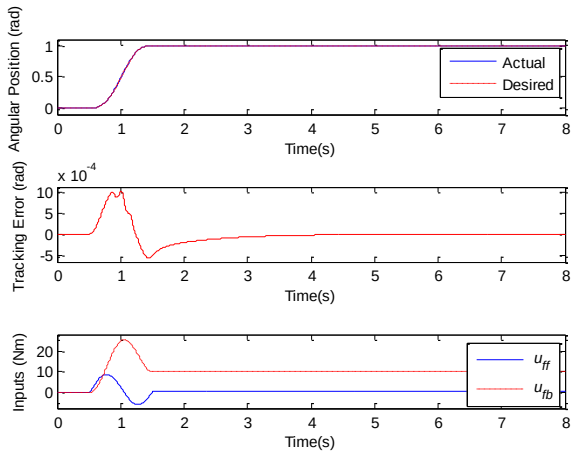

Figure 12. Top: Actual position θ_a and desired position θ_d. Middle: Tracking error $\theta_a - \theta_d$. Bottom: Inputs, using feedback control and feedforward control, I =1.2 kgm^2, T = 1 s.

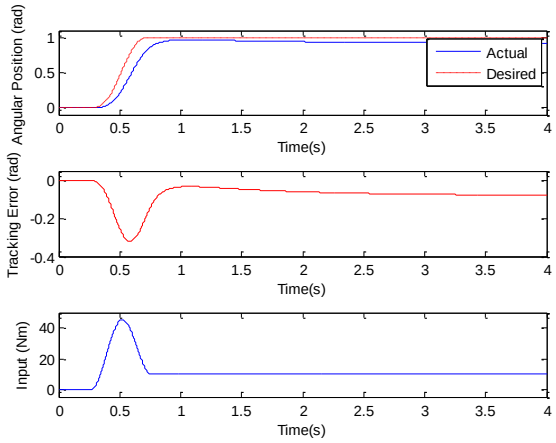

Figure 13. Top: Actual position θ_a and desired position θ_d. Middle: tracking error $\theta_a - \theta_d$. Bottom: Input, using feedback control alone, I =1.0 kgm^2, T = 0.5 s.

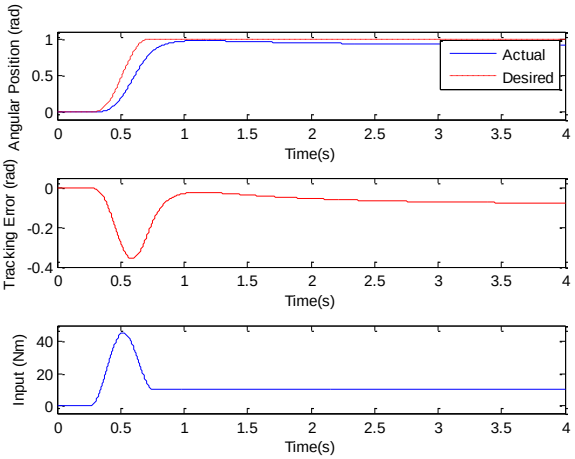

Figure 14. Top: Actual position θ_a and desired position θ_d. Middle: Tracking error $\theta_a - \theta_d$. Bottom: Input, using feedback control alone, I =1.2 kgm^2, T = 0.5 s.

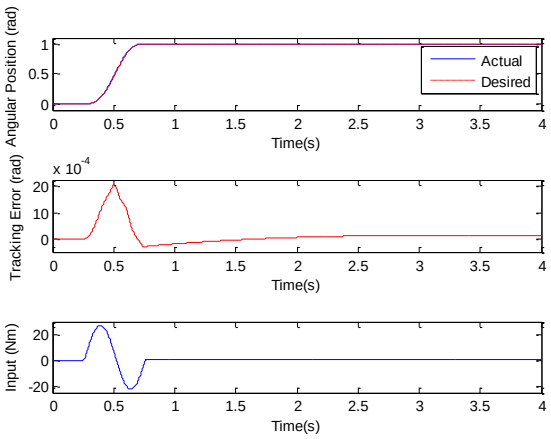

Figure 15. Top: Actual position θ_a and desired position θ_d. Middle: Tracking error $\theta_a - \theta_d$. Bottom: Input, using feedforward control alone, I =1.0 kgm^2, T = 0.5 s.

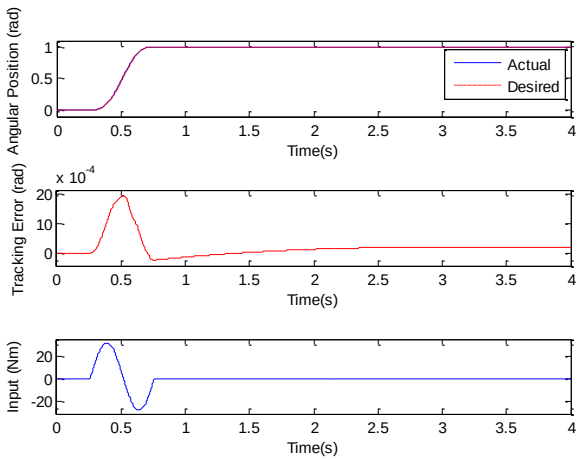

Figure 16. Top: Actual position θ_a and desired position θ_d. Middle: Tracking error $\theta_a - \theta_d$. Bottom: Input, using feedforward control alone, I =1.2 kgm^2, T = 0.5 s.

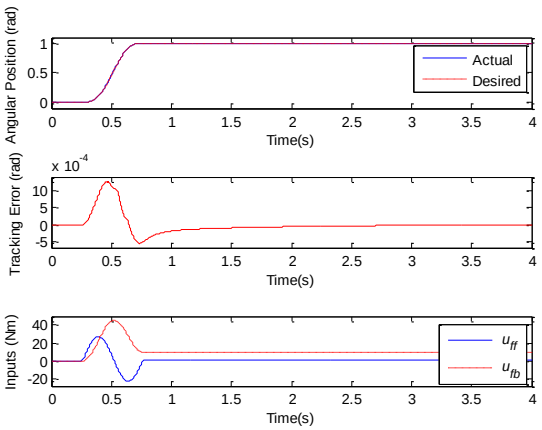

Figure 17. Top: Actual position θ_a and desired position θ_d. Middle: Tracking error $\theta_a - \theta_d$. Bottom: Inputs, using feedback control and feedforward control, I =1.0 kgm^2, T = 0.5 s.

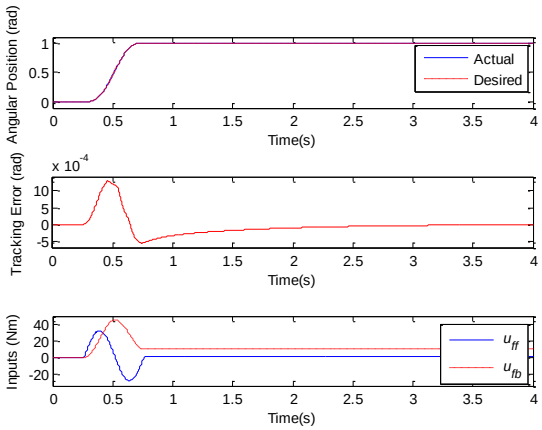

Figure 18. Top: Actual position θ_a and desired position θ_d. Middle: Tracking error $\theta_a - \theta_d$. Bottom: Inputs, using feedback control and feedforward control, I =1.2 kgm^2, T = 0.5 s.

A. *Quantifying the Tracking Errors*

The numerical evaluation of tracking can be made by using the tracking error, *E(t)*,which can be defined as

$$E(t) = \theta_a(t) - \theta_d(t) \tag{27}$$

where $\theta_a(t)$ denotes the actual trajectory output, and $\theta_d(t)$ represents the desired trajectory output. *E(t)* is shown in the middle figures of Fig. 7 to Fig.18.

The performance of tracking can also be quantified by the maximum tracking error $E_{\max}$, which is defined by

$$E_{\max} = \max|E(t)| \tag{28}$$

To examine the overall tracking performance for the whole tracking time, *RMSE*, or root mean square error, can be used as a performance index of trajectory tracking, and the *RMSE* is defined as

$$RMSE = \sqrt{\frac{1}{N}\sum_{i=1}^{N}(\theta_a(t) - \theta_d(t))^2} \tag{29}$$

where *N* denotes the number of the data points.

In addition, the percent tracking error can be defined as

$$E_{\text{percent}} = (\max|E(t)|/\theta_{\max})(100) \tag{30}$$

Here, $\theta_{\max} = 1\,\text{rad}.$

B. *Tracking Performance*

TABLE I. TRACKING ERRORS FROM DIFFERENT CONTROL APPROACHES WITH I =1.0 KGM^2, AND T = 1 S

Control Approaches	Tracking Errors		
	$E_{\max}$ (rad)	*RMSE* (rad)	Percent Error
Feedback	1.88x10^{-1}	7.81x10^{-2}	18.80
Feedforward	2.00x10^{-3}	5.45x10^{-4}	0.20
Feedback and Feedforward	1.00x10^{-3}	2.27x10^{-4}	0.10

TABLE II. TRACKING ERRORS FROM DIFFERENT CONTROL APPROACHES WITH I =1.2 KGM^2, AND T = 1 S

Control Approaches	Tracking Errors		
	$E_{\max}$ (rad)	*RMSE* (rad)	Percent Error
Feedback	2.13x10^{-1}	8.02x10^{-2}	21.32
Feedforward	2.00x10^{-3}	5.68x10^{-4}	0.20
Feedback and Feedforward	1.00x10^{-3}	2.35x10^{-4}	0.10

TABLE III. TRACKING ERRORS FROM DIFFERENT CONTROL APPROACHES WITH I =1.0 KGM^2, AND T = 0.5 S

Control Approaches	Tracking Errors		
	$E_{\max}$ (rad)	*RMSE* (rad)	Percent Error
Feedback	3.20x10^{-1}	9.39x10^{-2}	32.00
Feedforward	2.00x10^{-3}	5.56x10^{-4}	0.20
Feedback and Feedforward	1.30x10^{-3}	2.76x10^{-4}	0.13

TABLE IV. TRACKING ERRORS FROM DIFFERENT CONTROL APPROACHES WITH I =1.2 KGM^2, AND T = 0.5 S

Control Approaches	Tracking Errors		
	$E_{\max}$ (rad)	*RMSE* (rad)	Percent Error
Feedback	3.58x10^{-1}	1.00x10^{-1}	35.84
Feedforward	1.90x10^{-3}	6.32x10^{-4}	0.19
Feedback and Feedforward	1.20x10^{-3}	3.12x10^{-4}	0.12

Fig. 7 to Fig. 18 and Table I to Table IV show that (i) using the feedback control alone cannot yield good tracking, and tracking with the feedback control alone gets worse when the trajectory gets faster, or there is a modeling error, or perturbation in the system, (ii) using the feedforward control alone can substantially improve the tracking although the trajectory gets faster, or there is a modeling error, or perturbation in the system, and (iii) the integration, or combination of the feedforward control scheme with the feedback control approach can further improve the tracking and can achieve the best tracking performance. The combined controller can produce good tracking of the fast system under perturbations.

V. CONCLUSIONS

This work seeks control approaches to controlling the motion of a robotic arm that needs to follow a given time-profile trajectory within a required time. The equation of motion of the robotic arm is derived and it exhibits a nonlinear behavior. This article proposes three different control methods: (i) feedback control approach, (ii)

inversion-based feedforward control, and (iii) integration, or combination of feedback control method with inversion-based feedforward control approach. Each control approach is simulated to track time-profile trajectories. The study also includes the tracking under perturbations, or modeling errors and the tracking of faster trajectories. The tracking performance for each controller is evaluated through tracking errors. The tracking results show that (i) using the feedback control alone cannot yield good tracking, and tracking with the feedback control alone gets worse when the trajectory gets faster, or there is a modeling error, or perturbation in the system, (ii) applying the feedforward method alone can substantially improve the tracking although the trajectory gets faster, or there is a modeling error, or perturbation in the system, and (iii) the integration, or combination of feedback control method with inversion-based feedforward control approach can further improve the tracking and can achieve the best tracking performance. The combined controller can produce good tracking of the fast system under perturbations.

The future work would investigate the effects of input saturations on the tracking performances.

ACKNOWLEDGMENT

This research work is supported by Assumption University of Thailand.

REFERENCES

[1] M. Beschi, S. Dormido, J. Sanchez ,A., Visioli, and L. J, "Event-based PI plus feedforward control strategies for a distributed solar collector field," *IEEE Transactions on Control Systems Technology*, vol. 23, no. 4, pp. 1615–1622, July 2014.

[2] P. Martin, S. Devasia, and B. Paden, "A different look at output tracking: Control of a VTOL aircraft," *Automatica*, vol. 32, no. 1, pp. 101-107, January 1994.

[3] J. Kongthon and S. Devasia, "Feedforward control of piezoactuator for evaluating cilia-based micro-mixing," in *Proc. 18th IFAC World Congress, IFAC 2011*, Milan, Italy, August 28-September 2, 2011, pp. 12727-12732.

[4] J. Kongthon and S. Devasia, "Iterative control of Piezoactuator for evaluating biomimetic, Cilia based Micromixing," *IEEE/ASME Transactions on Mechatronics*, vol.18, no. 3, June 2013, pp. 944-953.

[5] J. Kongthon, "Tracking of high-speed, non-smooth, and microscale-amplitude wave trajectories," in *Proc. 2016 13th International Conference on Informatics in Control, Automation and Robotics (ICINCO 2016*), July 2016, pp. 499-507.

[6] J. Kongthon, N. S. Mosley, and R. E. Farrell, "Time scaling for motion control of a high-order and very fast dynamic system," *IEEE Proceedings of 2nd International Conference on Control and Robotics Engineering (ICCRE2017)*, Bangkok, Thailand, April 1-3,2017,pp.124-129.

[7] J. Kongthon, "Modeling and control of flexible structure systems with lumped masses," *IEEE Proceedings of 2017 8th International Conference on Mechanical and Aerospace Engineering (ICMAE 2017)*, Prague, Czech Republic, July 22-25, 2017, pp. 228-233.

[8] S. Zribi, H. Tlijani, J. Knani, and V. Puig, "Improvement of ultra-local model control using the auto-tuning PID control applied to redundant manipulator robot," *International Journal of Mechanical Engineering and Robotics Research*, vol. 8, no. 1, pp. 25-30, January 2019.

[9] V. H. L. Enr ́quez and V. G. Alejo, "Hybrid force-position control for manipulators under transitions free to constrained motion," *International Journal of Mechanical Engineering and Robotics Research*, vol.4, no. 4, pp. 319-324, October 2015.

[10] M. Galicki, "Finite-time control of robotic manipulators," *Automatica*, vol. 51, pp. 49-54, January 2015.

[11] T. Meng and W. He, "Iterative learning control of a robotic arm experiment platform with input constraint," *IEEE Transactions on Industrial Electronics* ,vol. 65, no. 1, pp. 664-672, January, 2018.

[12] J. J. E. Slotine and W. Li, *Applied Nonlinear Control*, Prentice-Hall, 1991, ch.6, pp. 246-248.

[13] D. E. Miller, "A comparison of LQR optimal performance in the decentralized and centralized settings," *IEEE Transactions on Automatic Control*, vol.61, no. 8, pp. 2308 – 2311, August 2016.

[14] S. Skogestad and I. Postlethwaite, *Multivariable Feedback Control: Analysis and Design*,Wiley, 2nd Ed., November 4, 2005, ch.9, pp. 344-346.

[15] L. M. Silverman, "Inversion of multivariable linear systems," *IEEE Transactions on Automatic Control*, vol. AC-14, no. 3, June 1969, pp. 270-276.

[16] R. M. Hirschorn. "Invertibility of multivariable nonlinear control systems," *IEEE Transactions on Automatic Control*, vol. AC-24, no. 6, pp. 855-865, December,1979.

[17] E. Davison, "The steady-state invertibility and feedforward control of linear time-invariant systems," *IEEE Transactions on Automatic Control*, vol. 21 , no. 4 , pp. 529 – 534, August 1976.

[18] S. Devasia, "Should model-based inverse inputs be used as feedforward under plant uncertainty?" *IEEE Transactions on Automatic Control*, vol. 47, no. 11, pp. 1865-1871, November 2002.

[19] A. Piazzi and A. Visioli, "Optimal inversion-based control for the setpoint regulation of nonminimum-phase uncertain scalar systems," *IEEE Transactions on Automatic Control*, vol. 46, no. 10, pp. 1654–1659, October 2001.

[20] X. Yang, M. Garratt, and H. Pota, "Flight validation of a feedforward gust-attenuation controller for an autonomous helicopter," *Robotics and Autonomous Systems*, vol. 59, no. 12, pp. 1070–1079, December 2011.

[21] P. H. Meckl and R. Kinceler, "Robust motion control of flexible systems using feedforward forcing functions," *IEEE Transactions on Control Systems Technology*, vol. 2, no. 3, pp. 245–254, September 1994.

[22] J. Hu and J. F. Lin,"Feedforward active noise controller design in ducts without independent noise source measurements," *IEEE Transactions on Control Systems Technology*, vol. 8, no. 3, pp. 443 - 455, May 2000.

[23] F. Dunn, L. Y. Pao, A. D. Wright, B. Jonkman, and N. Kelley, "Adding feedforward blade pitch control to standard feedback controllers for load mitigation in wind turbines," *Mechatronics*, vol. 21, no. 4, pp. 682–690, June 2011.

Jiradech Kongthon received a Bachelor of Engineering in Mechanical Engineering from King's Mongkut University of Technology Thonburi, Thailand. He earned a Master of Science in Engineering Management with Distinction from California State University, Northridge in 2002 and a Master of Science in Aerospace and Mechanical Engineering from University of Southern California, Los Angeles in 2006. In 2011, he received a PhD degree in Mechanical Engineering from the University of Washington in Seattle,USA and worked as a Research Associate at the University of Washington till 2012.

Jiradech Kongthon is currently with Assumption University of Thailand and works as an Associate Professor in the department of Mechatronics Engineering. His current research interests include dynamic systems, modeling, control, air-conditioning systems, climate control systems, and green building technologies.